Malignant Pleural Mesothelioma Caused by Environmental Exposure to Asbestos or Erionite in Rural Turkey: CT Findings in 84 Patients

Ahmet Altay Şahin[1]
Lütfü Çöplü[1]
Ziya Toros Selçuk[1]
Muzaffer Eryılmaz[2]
Salih Emri[1]
Okhan Akhan[2]
Yusuf İzzettin Barış[1]

OBJECTIVE. Malignant pleural mesothelioma in rural Turkey frequently results from environmental exposure to tremolite asbestos or fibrous zeolite (erionite). The aim of this study was to determine the CT features of malignant pleural mesothelioma in patients exposed to asbestos or erionite.

MATERIALS AND METHODS. The CT scans of 84 patients with proved malignant pleural mesothelioma were retrospectively evaluated. Twenty patients (24%) had been exposed to erionite and 64 patients (76%) had been exposed to asbestos. The CT scans were interpreted by seven observers who did not know the clinical or pathologic findings.

RESULTS. CT scans showed either unilateral pleural thickening or pleural nodules/masses in all patients. Pleural nodules were present in 25 patients (30%) and pleural masses in 44 patients (52%). Pleural effusion was found in 61 patients (73%), mediastinal pleural involvement in 78 (93%), pleural calcifications in 52 (62%), involvement of the interlobar fissures in 64 (76%), and volume contraction in 61 (73%). Reduced size of the hemithorax was significantly correlated with chest wall involvement. On the basis of CT findings, the preassigned staging was changed in 21 patients (25%), including 44% of the patients with disease that had been classified as stage I. CT findings were not significantly different between the patients exposed to erionite and those exposed to asbestos.

CONCLUSION. The most common CT findings in cases of malignant pleural mesothelioma were unilateral pleural thickening or pleural nodules/masses with or without effusion. CT provided valuable information on the extent of the disease, which was important for staging. Although the CT features are not pathognomonic, they provide valuable clues to the diagnosis in patients who have been exposed to mineral fibers.

AJR **1993;161:533–537**

Malignant pleural mesothelioma commonly occurs in patients born or living in certain villages in central and southeastern Turkey. Previous environmental studies in rural parts of the country revealed mainly tremolite asbestos in the villages where pleural mesothelioma occurred [1–4]. Unlike malignant pleural mesothelioma caused by occupational exposure, frequently from crocidolite or amosite asbestos, mesothelioma caused by environmental exposure in Turkey, Greece, and Cyprus is most often due to tremolite asbestos [1–7]. White stucco that is contaminated with tremolite asbestos is used to insulate the roofs and plaster walls of houses in rural Turkey. Another mineral, erionite, is a known cause of malignant mesothelioma in three villages in central Turkey [8–10]. This mineral, one of the natural fibrous zeolites, is an environmental contaminant originating from the volcanic rocks on which these three villages are built. Neither erionite nor asbestos is commercially exploited in Turkey. Asbestos is the most common fibrous mineral responsible for malignant mesothelioma, but erionite is the most potent.

We report the CT findings in 84 cases of malignant pleural mesothelioma caused by environmental exposure to tremolite asbestos or erionite.

Received January 5, 1993; accepted after revision April 19, 1993.

[1]Department of Chest Diseases, Hacettepe University, School of Medicine, Sıhhiye 06100, Ankara, Turkey. Address correspondence to A. Sahin.

[2]Department of Radiology, Hacettepe University, School of Medicine, Ankara, Turkey.

0361–803X/93/1613–0533

Materials and Methods

We retrospectively reviewed the CT scans of 84 patients (51 men and 33 women) with proved malignant pleural mesothelioma seen at Hacettepe University Hospitals, School of Medicine, Ankara, Turkey, between 1989 and 1992. The diagnoses of malignant mesothelioma were confirmed pathologically in all cases. The pathologic subtype of mesothelioma, where noted, was also included. The patients were divided into two groups according to geographic location. Twenty patients (24%) were from Karain, Tuzkoy, or Sarihidir in central Turkey, where residents are environmentally exposed to erionite. The other 64 patients (76%) lived in villages where inhabitants are environmentally exposed to asbestos. None of the patients had been occupationally exposed to asbestos. Disease was staged according to the system proposed by Butchard et al. [11], which is based on the clinical findings and results of radiologic studies. Stage I was defined as tumor confined to the ipsilateral parietal pleura. Stage II was defined as tumor involving the chest wall or mediastinal structures beyond the capsule of the pleura. Tumor penetrating the diaphragm with peritoneal involvement, contralateral pleural involvement, or lymph node involvement outside the chest was designated as stage III. Distant blood-borne metastases were classified as stage IV.

The mean and median ages of the 84 patients were 48 ± 11 years and 48 years, respectively, with an age range of 26–76 years. The differences between the mean ages of the erionite and asbestos groups and between men and women were not statistically significant (Student's t-test, $p > .05$ for both). Twenty-seven patients (32%) were smokers, eight (10%) had previously smoked, and 49 (58%) had never smoked. All women were nonsmokers. All but three patients (96%) had either chest pain or dyspnea.

In most patients, the diagnosis of malignant pleural mesothelioma was made by either closed pleural biopsy (44%), thoracoscopy (27%), or thoracotomy (21%). Sonographically guided percutaneous biopsy of the pleural lesions was used to confirm the diagnosis in four cases, excisional biopsy of an extrathoracic soft-tissue lesion revealed mesothelioma in one patient, and CT-guided percutaneous biopsy of the pleura did so in another. Of the subtypes of mesothelioma reported in 48 patients (57%), 45 (94%) were classified as epithelial (tubulopapillary) and three (6%) as mesenchymal (fibrosarcomatous).

The CT scans were obtained before any invasive procedure was done. Scans were made from the apex to the diaphragm with a 9-mm slice thickness and 4.8-sec scan time. Scans were obtained at end-inspiratory lung volumes with the patient supine. Both mediastinal and parenchymal window settings were used. Scans obtained outside our institution also were included. The CT scans were evaluated by a panel of five chest physicians and two radiologists, none of whom knew the clinical or pathologic findings. A consensus was sought in cases of disagreement. On CT scans, pleural thickening was defined as a pleural thickness of 10 mm or less, pleural nodules as focal pleural thickness of no more than 10–30 mm, and pleural masses as pleura-based soft-tissue masses with diameters of 30 mm or more. The involvement of interlobar fissures was noted, and abnormalities of the fissures were also classified as pleural nodules or masses. The effusions were considered massive if they occupied more than half of the hemithorax. The presence of calcified pleural plaques and hyaline pleural plaques on the contralateral pleura also was assessed. Hyaline pleural plaques were defined as a focal increase in soft-tissue density along the pleura, which is well demarcated and clearly separated from the lung [12, 13]. Because patients were not scanned while prone and high-resolution CT was not used, information regarding parenchymal lung disease was not included.

Student's t-test, χ^2-test, and Fisher's exact test were used for analysis of the results. We considered p values less than .05 as statistically significant.

Results

At presentation, each patient had only one hemithorax affected by the disease, the right (51 patients) more frequently than the left (33 patients). The pleura of the lower half of the hemithorax was more frequently involved than the pleura of the upper half (54 vs 30). Disease was classified as stage I in 39 patients (46%), stage II in 25 patients (30%), and stage III in 15 patients (18%). Five patients (6%) had distant metastases and were categorized as having stage IV disease.

Either pleural thickening or pleural nodules/masses were observed on CT scans obtained at presentation in all patients (Fig. 1). Unilateral pleural thickening was detected

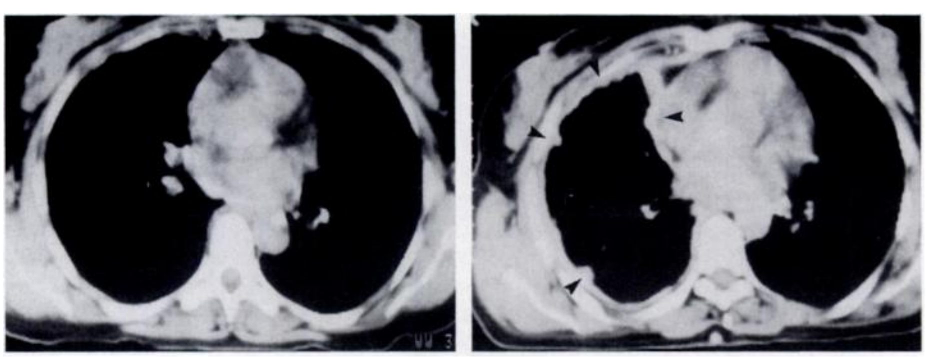

A B

Fig. 1.—50-year-old woman with previous environmental exposure to asbestos.

***A*, CT scan obtained because of vague chest discomfort shows normal findings.**

***B*, CT scan at approximately same level 2 years later shows irregular thickening of mediastinal and costal pleura (*arrowheads*) and volume loss of right hemithorax. Assessment of pericardial invasion was difficult because of contiguous pleural involvement. Malignant pleural mesothelioma was diagnosed by pleural biopsy.**

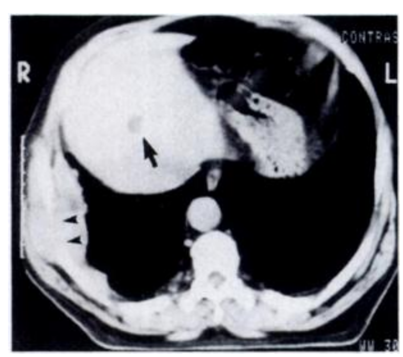

Fig. 2.—55-year-old man previously exposed to erionite. CT scan shows irregular pleural masses at lateral and paravertebral portions of right hemithorax. Chest wall invasion with rib destruction in lateral portion is evident (*arrowheads*). Hyperdense round lesion (*arrow*) in right hepatic lobe is presumed to be a solitary metastasis. Malignant mesothelioma was diagnosed by thoracotomy.

in 78 patients (93%), and the pleuropulmonary margin was irregular in 78 patients (93%) (Table 1). Either focal or multiple pleural soft-tissue lesions were noted in 69 patients (82%), of whom 25 had pleural nodules and 44 had pleural masses. Associated extrathoracic soft-tissue lesions were present in 18 patients (21%) (Fig. 2). Circumferential pleural masses encased the pulmonary parenchyma completely or almost completely in 36 patients (43%). Pleural effusion accompanied the mass lesions in 46 patients (55%). The interlobar fissures were involved in 64 patients (76%) (Fig. 3). The pleural fissures were thickened in 34 (53%) of these, masses or nodules were present in 28 (44%), and both findings were present in two patients. Pleural effusion was present in 61 patients (73%); it was massive in 24 patients (Fig. 4) and moderate in 37. The frequency of moderate or massive pleural effusion was not significantly different between the asbestos and erionite groups (χ^2-test, $p > .05$ for both). The diaphragm was inverted because of a pleural effusion on the left side in 13 patients and on the right side in three patients.

TABLE 1: CT Findings in 84 Patients with Malignant Pleural Mesotheliomas

CT Finding	No. (%) of Cases
Pleural thickening	78 (93)
Irregular pleural margin	78 (93)
Mediastinal pleural thickening	78 (93)
Interlobar fissural involvement	64 (76)
Volume contraction	61 (73)
Pleural effusion	61 (73)
Calcified pleural plaques	52 (62)
Pleural masses	44 (52)
Rindlike thickening	36 (43)
Pleural nodules	25 (30)
Contralateral hyaline plaques	22 (26)
Rib erosion	16 (19)
Contralateral fissural thickening	11 (13)
Rounded atelectasis	6 (7)
Liver metastases	5 (6)
Chest hypertrophy	3 (4)
Vertebral body erosion	3 (4)
Pneumothorax	3 (4)

Involvement of the mediastinal pleura was noted in 78 patients (93%). The pericardium also was thickened in 60 (77%) of these cases. Mediastinal lymphadenopathy accompanied pleural thickening in 43 patients. The mediastinum remained midline in 30 patients (36%), seven of whom had unilateral massive effusions. The mediastinum was displaced to the contralateral side in 14 patients who had massive effusions and in four who had moderate effusions. The mediastinum was retracted to the ipsilateral side in 36 patients (43%), 15 of whom did not have an effusion and three of whom had massive effusions. Mediastinal involvement by the tumor was delineated with CT in six of the seven patients with the mediastinum in the midline and in all three patients who had ipsilateral shift of the mediastinum in the presence of massive pleural effusions.

The affected hemithorax was contracted in 61 patients (73%), all of whom showed rib crowding (Fig. 5). Contraction of the hemithoraces was noted at physical examination in 25 (41%) and on chest radiographs in 49 (80%) of the 61 patients. Volume reduction was present in all cases except for one patient who had chest wall involvement (χ^2-test, Yates' corrected, $p < .05$). Pleural effusions accompanied the volume contraction in 40 patients, 12 of whom had massive effusions. Among the 61 patients with volume contraction, the mediastinum was pulled to the ipsilateral side in 33 (54%), remained midline in 20 (33%), and was pushed to the contralateral side in eight (13%). The affected hemithorax had increased volume compared with the contralateral side in three patients with massive effusions and contralateral shift of the mediastinum. Pleural nodules and masses were reported in one case each. In none of these patients did our review find that volume contraction of the affected hemithorax continued throughout the course of the disease.

Five patients had distant blood-borne metastases to the liver at presentation. In eight patients, pulmonary nodules were noted on CT scans at the time of diagnosis that were regarded as pulmonary metastases (Fig. 6). Histologic confirmation was not available in these patients. Destructive mass lesions within the extrathoracic tissues were delineated on CT scans of 19 patients. These lesions eroded the ribs in 13 patients and the ribs and the vertebral bodies in another three.

Calcified pleural plaques were evident on CT scans of 52 patients (62%) and were bilateral in 19 of these (Fig. 3). The

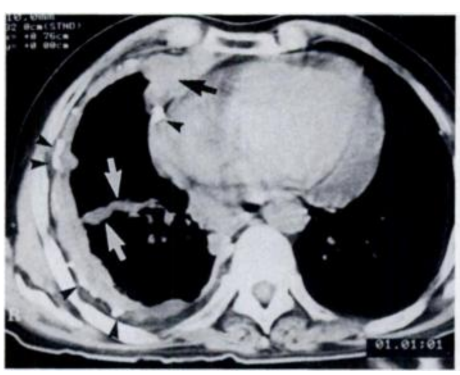

3

4

Fig. 3.—50-year-old man exposed to asbestos. CT scan shows diffuse irregular thickening involving all portions of pleura and a mass at right cardiophrenic angle (*black arrow*). Nodular lesions are visible in interlobar pleura (*white arrows*). Multiple calcifications (*arrowheads*) are visible in costal pleura, paravertebral region, and pericardium. Mediastinum is central. Malignant pleural mesothelioma was diagnosed by pleural biopsy.

Fig. 4.—36-year-old man exposed to asbestos. CT scan shows multiple pleural masses (*arrows*) and massive pleural effusion (*asterisks*) resulting in atelectasis of underlying lung (*arrowheads*). Diagnosis was confirmed by thoracoscopy.

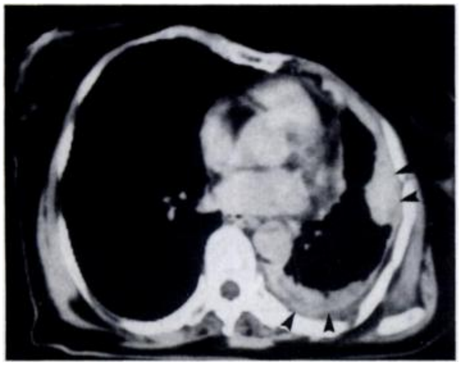

5

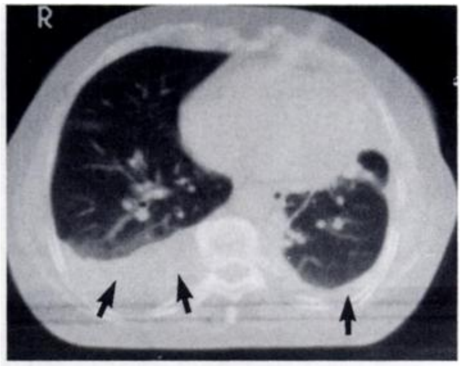

6

Fig. 5.—57-year-old woman with malignant pleural mesothelioma who had been exposed to erionite. CT scan shows volume loss of left hemithorax along with rib crowding. Pleural thickening and masses (*arrowheads*) involve all pleural surfaces. Mediastinum is pulled to left side. Pleural biopsy revealed malignant mesothelioma.

Fig. 6.—61-year-old woman who had been exposed to asbestos in childhood. Malignant pleural mesothelioma was confirmed by thoracoscopy. Follow-up CT scan shows bilateral pleural effusions (*arrows*), volume loss of left hemithorax, ipsilateral mediastinal shift, and bilateral multiple pulmonary nodules presumed to be metastases.

plaques were observed in 11 of the 20 patients exposed to erionite and in 41 of the 64 exposed to asbestos. The frequencies of either unilateral or bilateral calcified plaques were not significantly different between the erionite and asbestos groups (χ^2-test, $p > .05$; Fisher's exact test, $p > .05$). Hyaline plaques on the contralateral side were shown in 22 patients (26%); thickening of the interlobar fissures was shown in 11 (13%), and calcified plaques were noted in six of these. Rounded atelectasis diagnosed via history of pleural fluid accumulation and appropriate radiologic follow-up was diagnosed in six patients.

CT findings changed the staging of disease in 17 patients in whom stage I disease had been diagnosed previously. This represents 44% of the patients in whom stage I disease was diagnosed. Disease was reclassified as stage II in 12 patients, as stage III in three, and as stage IV in two. In one patient with stage II disease, stage III disease also was diagnosed. In two patients with disease classified as stage II and in one with disease classified as stage III on the basis of clinical and chest radiographic findings, stage IV disease was diagnosed on the basis of the presence of liver metastases. Sonography showed abdominal extension in all eight patients with stage III disease and liver metastases in five patients with stage IV disease.

Discussion

CT evidence of the extent of disease and the CT appearance of the malignant pleural mesothelioma varied considerably, as was the case in previously reported series [14–17]. The most common CT findings were unilateral pleural thickening and irregular pleuropulmonary contour. CT is more accurate than chest radiography for showing the extent of the disease, thus affording more reliable staging and appropriate treatment decisions [15, 16, 18–20]. CT contributed to staging of disease in one fourth of the patients in this series. In 17 (44%) of the patients in whom the disease was initially classified as stage I, the disease was reclassified to a higher stage on the basis of CT findings.

We noted that volume contraction was assessed better and sooner with CT than with physical examination or chest radiography. Volume contraction was present in almost all patients in whom the lung was encased circumferentially by tumor (34 of 36 patients) (Fig. 7). Contraction was also a typical feature in almost all patients with chest wall involvement.

CT was helpful for determining the best site for biopsy in some of the patients with pleural masses. CT or sonographically guided biopsies were successful in four of the five patients in whom these techniques were used; in one, repeated sonographically guided percutaneous pleural biopsy provided the diagnosis subsequently.

Chest wall invasion was not detected preoperatively on CT scans but was noted at thoracotomy in three of the 18 patients who had surgery. These results are in agreement with those of Rusch et al. [20], who stated that chest wall involvement in mesothelioma is underestimated when CT is used. CT provides limited information about mediastinal lymph node and chest wall involvement, peritoneal metastases, and transdiaphragmatic extension [20]. We assume that volume loss suggests chest wall involvement in patients with a presumptive diagnosis of pleural mesothelioma, even though the CT findings are equivocal. Pericardial thickening is also not a specific finding and may be from either tumor invasion or fibrosis [18]. Assessment of pericardial invasion and mediastinal lymphadenopathy was difficult in our series because of contiguous mediastinal pleural involvement.

CT evidence of previous exposure to mineral fibers, such as hyaline pleural plaques, calcified pleural plaques, or rounded atelectasis, was found often in patients in this series. This may be because exposure occurred at an early age and the disease has a long latent period, even though the exposure might not have been extensive [9]. In fact, we assume that the presence of any one of these signs is a radiologic clue to the diagnosis of pleural mesothelioma in a patient with unilateral pleural disease or effusion. Calcification is less prevalent in mesothelioma than in asbestosis, but it does occur in cases of pleural mesothelioma [14, 19]. Calcified pleural plaques are better assessed on CT scans than on chest radiographs; chest radiographs showed the plaques in only 16 (31%) of the 52 patients with calcified plaques. The frequencies of these benign pleural changes were not different between the two groups of minerals.

None of the CT features described in other reports or in this series is pathognomonic for malignant pleural mesothelioma [15, 19]. The differential diagnosis includes metastatic

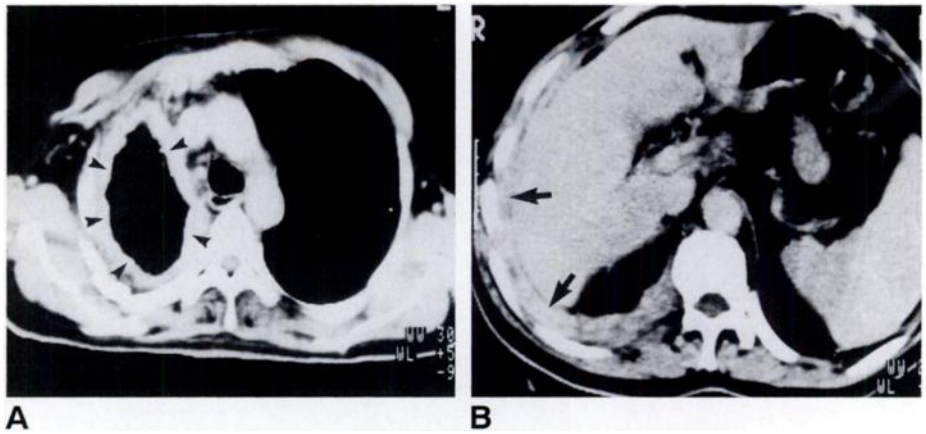

Fig. 7.—44-year-old man with a history of environmental asbestos exposure.

***A*, CT scan shows pleural rind (*arrowheads*) encasing lung with prominent volume loss and rib crowding.**

***B*, CT scan at subdiaphragmatic level shows abdominal extension of diffusely thickened irregular pleura on posterolateral aspect of liver (*arrows*). Mesothelioma was diagnosed by thoracotomy.**

carcinoma of the pleura, bronchial carcinoma, lymphoma, and pleural asbestosis [15, 18, 19, 21]. Although pleural lesions are usually smooth and localized in asbestosis, it may not be possible to distinguish between pleural plaques and mesothelioma [17–19]. In countries with a high prevalence of pleural tuberculosis, that disease should be considered in the differential diagnoses because of similar radiographic findings [22]. A history of exposure to mineral fibers is the most valuable clue to the nature of the lesions seen on CT scans.

Reports of patients with malignant pleural mesothelioma generally include patients with asbestos-related malignant pleural mesotheliomas from occupational exposure. Erzen et al. [17] reported the CT findings in patients with environmental exposure to asbestos and erionite. The prevalence of bilateral disease and transdiaphragmatic extension was higher in the erionite-related pleural mesothelioma group than in the asbestos-related group. Stage III disease was more common among patients exposed to asbestos, and stage IV was more common among patients exposed to erionite. These differences were not apparent in our series of 84 patients with erionite- and asbestos-related pleural mesothelioma. These differences may be due to the late presentation of patients with erionite-related pleural mesothelioma in the previous study.

In conclusion, our results indicate that CT findings in cases of malignant pleural mesothelioma vary. Although some findings are quite characteristic, none is pathognomonic for the disease. However, CT findings in patients who have been exposed to mineral fibers provide valuable clues to the diagnosis. In Turkey, the place of birth or residence of patients determines if environmental exposure to either erionite or asbestos has occurred. We also noted that CT findings in patients with malignant pleural mesothelioma caused by erionite exposure were not significantly different from those in patients with mesothelioma caused by asbestos exposure.

REFERENCES

1. Barış Yİ, Artvinli M, Şahin AA. Environmental mesothelioma in Turkey. *Ann N Y Acad Sci* **1980**;330:423–432
2. Yazıcıoglu S, Oktem K, Ilcayto R, Balcı K, Saylı BS. Association between malignant tumours of the lung and pleurae and asbestosis. *Chest* **1978**;73:52–56
3. Barış Yİ. *Asbestos and erionite related chest diseases*. Ankara: Semih Ofset Matbaacılık, **1987**:62–109
4. Barış Yİ, Bilir N, Artvinli M, Şahin AA, Kalyoncu F, Sebastian F. An epidemiological study on an Anatolian village environmentally exposed to tremolite asbestos. *Br J Ind Med* **1988**;45:838–840
5. Selçuk ZT, Çöplü L, Emri S, Kalyoncu AF, Şahin AA, Barış Yİ. Malignant pleural mesothelioma due to environmental mineral fiber exposure in Turkey: analysis of 135 cases. *Chest* **1992**;102:790–796
6. Constantopoulos SH, Theodoracopoulos P, Dascalopoulos G, Saratzis N, Sideris K. Metsovo lung outside Metsovo: endemic pleural calcifications in the ophiolite belts of Greece. *Chest* **1991**;99:1158–1161
7. McConnochie K, Simonato L, Mavrides P, Christofides P, Pooley FD, Wagner JC. Mesothelioma in Cyprus: the role of tremolite. *Thorax* **1987**; 42:342–347
8. Barış Yİ, Saracci R, Simonoto L, Skidmore JW, Artvinli M. Malignant mesothelioma and radiological chest abnormalities in two villages in central Turkey. *Lancet* **1981**;1:984-987
9. Barış Yİ, Simonato L, Artvinli M, et al. Epidemiological and environmental evidence of the health effects of exposure to erionite fibers: a four-year study in the Cappadocian region of Turkey. *Int J Cancer* **1987**;39:10-17
10. Barış Yİ. Fibrous zeolite (erionite)-related diseases in Turkey. *Am J Indust Med* **1991**;19:374–378
11. Butchard EG, Ashcroft T, Barnsley WC, Holden MP. Pleuropneumonectomy in the management of diffuse malignant mesothelioma of the pleura. *Thorax* **1976**;31:15–24
12. Hillerdal G. Asbestos-related pleural disease. *Semin Respir Med* **1987**;9: 65–74
13. Lynch DA. Imaging of asbestos-related thoracic disease. *Semin Respir Med* **1992**;13:332–344
14. Kawashima A, Libshitz HI. Malignant pleural mesothelioma: CT manifestations in 50 cases. *AJR* **1990**;155:965–969
15. Alexander E, Clark RA, Colley DP, Mitchell SE. CT of malignant pleural mesothelioma. *AJR* **1981**;137:287–291
16. Mirvis S, Dutcher JP, Haney PJ, Whitley NO, Aisner J. CT of malignant pleural mesothelioma. *AJR* **1983**;140:665–670
17. Erzen C, Eryılmaz M, Kalyoncu F, Bilir N, Şahin A, Barış Yİ. CT findings in malignant pleural mesothelioma related to nonoccupational exposure to asbestos and fibrous zeolite (erionite). *J Comput Assist Tomogr* **1991**; 15:256–260
18. Grant DC, Seltzer SE, Antman KH, Finberg HJ, Koster K. Computed tomography of malignant pleural mesothelioma. *J Comput Assist Tomogr* **1983**;7:626–632
19. Rabinowitz JG, Efremidis SC, Cohen B, et al. A comparative study of mesothelioma and asbestosis using computed tomography and conventional chest radiography. *Radiology* **1982**;144:453–460
20. Rusch VW, Godwin JD, Shuman WP. The role of computed tomography scanning in the initial assessment and the follow-up of malignant pleural mesothelioma. *J Thorac Cardiovasc Surg* **1988**;96:171–177
21. Leung AN, Müller NL, Miller RR. CT in differential diagnosis of diffuse pleural disease. *AJR* **1990**;154:487–492
22. Hulnick DH, Naidich DP, McCauley DI. Pleural tuberculosis evaluated by computed tomography. *Radiology* **1983**;149:759–765